Renewable Energy 50 (2013) 395–401

Contents lists available at SciVerse ScienceDirect

Renewable Energy

journal homepage: www.elsevier.com/locate/renene

The extractable power from a split tidal channel: An equivalent circuit analysis

Patrick F. Cummins*

Institute of Ocean Sciences, Fisheries and Oceans Canada, Sidney, B.C., Canada V8L 4B2

ARTICLE INFO

Article history:
Received 19 September 2011
Accepted 3 July 2012
Available online 2 August 2012

Keywords:
Renewable energy
Tidal power
Resource assessment
Split channel
Electric circuit analogue

ABSTRACT

Considerable interest exists in the possibility of exploiting strong tidal currents as a source of renewable energy. Methods to understand and evaluate this resource have been developed for simple flow configurations, such as a tidal channel linking the open ocean to an inner basin. More complicated flow geometries involving branching channels have been considered recently. A simple prototype for this class of problem consists a tidal channel that is split by an island into two sub-channels. In-stream energy conversion devices are deployed in one of the sub-channels, while the second is left free for navigation or other purposes. The free sub-channel allows flow to be diverted away from the impeded sub-channel, which may lead to a reduction in the available power.

In the present paper, an electric circuit analogue is used to develop a linear theory for the power potential of a split tidal channel. Although limited to linear friction, this approach allows for inclusion of the effects of flow acceleration and finite basin size that have not been considered previously. Based on the equivalent circuit, analytical expressions are derived for the maximum extractable power and for the modification of the flow in each section of the channel at maximum power. Extension of the theory to multiple branching channels is discussed. Results for a few simple cases are considered.

1. Introduction

Renewable energy strategies depend on resource assessments to provide essential information regarding the power that is available to be exploited in a given natural setting. With respect to marine renewable energy, consideration has been given in recent years to deploying submarine turbines or other hydrokinetic devices in energetic tidal streams. Simple analytical models of the power potential of tidal flows have been developed that may be applied to estimate the resource and to help guide detailed assessments. Such models provide estimates of the maximum average power that may be extracted from the tidal motions. To date, only a few flow configurations have been considered. Greatest attention has been given to the case of a single tidal channel of variable cross-section that connects two large oceanic basins [1], or one that links the ocean to an inner basin of finite area [2–5]. To estimate the maximum extractable power, these studies assume that the flow is uniform across the channel and that all of it passes through a turbine 'fence' that spans the channel. Extensions of the theory have been considered to allow for fences that partially span a channel [6–8].

More complicated flow geometries have been considered recently [9,10]. A prototypical problem in this regard is that of the split tidal channel. In this configuration, an island divides the main channel into two branches, with energy conversion devices deployed in only one of the sub-channels. It is envisaged in such a scenario that one of the sub-channels is left open for ecological reasons, or for other purposes such as navigation. Atwater and Lawrence [9] considered the power potential of a split tidal channel connecting two oceanic basins of infinite extent. Their analysis allowed for quadratic drag, but was restricted to the frictional limit in which time dependence is neglected and the tidal head and volume flux are locked in phase. The power potential was estimated by maximizing the extraction efficiency, defined as the extracted power normalized by the net tidal energy flux into the channel, i.e., the dissipation in the undisturbed state. This is distinct from the maximum extractable power, although the two may be similar if the introduction of turbines does not greatly alter the overall dissipation within the entire channel.

In the present paper, the split channel problem is considered in terms of its equivalent electrical circuit. Such a technique has been used to examine harbour resonances [11], and it has been applied recently to study the tidal power that may be extracted from the

* Tel.: +1 2503636553; fax: +1 2503636746.
E-mail address: patrick.cummins@dfo-mpo.gc.ca.

0960-1481/$ – see front matter
http://dx.doi.org/10.1016/j.renene.2012.07.002

Severn estuary [12]. The electric circuit analogy is particularly useful in the present context as it permits elementary network theorems to be invoked, reducing the complexity of the analysis substantially. Although the method is limited to linear frictional drag, time dependence and the effects of finite basin area are readily taken into account. Moreover, the approach may be generalized to allow for multiple branching channels.

In the next section, the flow configuration of the split channel problem and its equivalent circuit are presented. Expressions are derived for the maximum power and the modification to the flows associated with the extraction of energy. A few special cases are considered in Section 3. The results are summarized in the concluding section.

2. Flow configuration and equivalent circuit

The flow configuration examined in this paper is illustrated in Fig. 1. There is a tidally varying forcing of amplitude a at the mouth of a channel that connects the open ocean to an inner basin of area A_B. Some distance from the mouth, the main channel is divided by an island into two sub-channels, one of which is spanned by a turbine fence that impedes the flow. It is assumed that all of the flow in the impeded sub-channel passes through the fence. The objective is to determine the maximum power that may be extracted from the tidal motions by the turbines. The presence of a free sub-channel allows for diversion of flow from the impeded sub-channel which may lead to a reduction in the available power.

A number of simplifying assumptions are made to construct the circuit analogue:

- The flow through each channel is assumed to be non-divergent. For this condition to hold, the channel lengths must be small compared to a tidal wavelength, and the basin area must be large relative to the area of the channels [1,3,5].
- There is a linear relation between the head and the transport for each section of the channel. Thus the dynamics are governed by a linearized one-dimensional momentum balance.
- The amplitude of the tidal forcing at the mouth of the channel is unaffected by the introduction of turbines in one of the sub-channels. This 'back effect' will be small provided the exterior region is large and deep [13]. In other cases, the back effect can be accommodated by including the radiation impedance of the exterior region in the equivalent circuit [12].
- The basin responds as a uniform reservoir. This requires the dimensions of the basin to be small compared to the distance long gravity waves propagate over a tidal period.

Assuming harmonic time dependence, the linearized momentum balance of the impeded sub-channel is

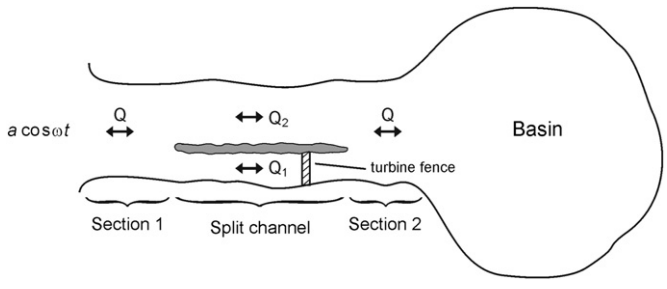

Fig. 1. Split channel flow configuration consisting of a tidal channel connecting the open ocean to a basin of area, A_B. An island located some distance from the mouth splits the channel into two branches. Energy extraction devices are deployed in a fence across one of the sub-channels while the other is left free.

$$i\omega u_1 = -g\frac{\partial \eta_1}{\partial x} - (r_1 + r_t)u_1 \tag{1}$$

where x is the along-channel coordinate, ω is the angular frequency, g is the acceleration due to gravity, $u_1(x)$ is the amplitude of the current, $\eta_1(x)$ is the sea level amplitude, $r_1(x)$ is the background frictional drag of the sub-channel, and $r_t(x)$ is the drag due to the turbines. A similar relation, but with turbine drag omitted, holds for free sub-channel. Although quadratic bottom drag is more realistic, assuming a linear drag law for bottom friction is necessary to obtain an analytical solution. An ad hoc method for taking some account of nonlinear drag is discussed in the concluding section. The influence of the turbines on the flow is also represented by a linear drag law. Experimental data suggest that this may, in fact, be more appropriate than a quadratic drag law [14]. Linear dynamics also eliminates the exit separation effect which may balance the head in short channels [1]. Integrating (1) along the length, ℓ_1, of the impeded sub-channel gives (cf. [1])

$$i\omega c_1 Q_1 = -g\Delta\eta - (\alpha_1 + \alpha_t)Q_1, \tag{2}$$

where $\Delta\eta$ is the elevation difference across the ends of the sub-channels, and $Q_1 = A_1 u_1$ is the (non-divergent) volume transport with $A_1(x)$ the cross-sectional area of the sub-channel. The constants in (2) are defined as

$$c_1 = \int_0^{\ell_1} A_1^{-1}\, dx, \tag{3a}$$

$$\alpha_1 = \int_0^{\ell_1} r_1 A_1^{-1}\, dx \tag{3b}$$

and

$$\alpha_t = \int_0^{\ell_1} r_t A_1^{-1}\, dx. \tag{3c}$$

With the usual analogy of voltage with pressure and electric current with volume transport (e.g., [15]), (2) can be expressed as $\Delta V = (Z_1 + R_L)I_1$, where the electric current $I_1 = Q_1$, and the voltage drop is $\Delta V = \rho g \Delta\eta$ with ρ the fluid density. The natural impedance of the channel, $Z_1 = R_1 + i\omega L_1$, includes a resistive component, $R_1 = \rho\alpha_1$ due to bottom frictional drag and an inductive component associated with flow acceleration, $\omega L_1 = \omega\rho c_1$. The load resistance, $R_L = \rho\alpha_t$, is associated with the drag of the turbine fence. A similar balance, $\Delta V = Z_2 I_2$, holds for the free sub-channel which has impedance, $Z_2 = R_2 + i\omega L_2$. Similarly, the impedance of the section of the main channel that lies between the mouth and island is $Z_{M1} = R_{M1} + i\omega L_{M1}$, while that between the island and basin is $Z_{M2} = R_{M2} + i\omega L_{M2}$. Relations analogous to (3a, b) determine the resistances and inductances for the free channel and the undivided sections of the main channel.

Fig. 2a presents the equivalent circuit for the flow configuration of Fig. 1. The voltage source has an amplitude $V_0 = \rho g a$. Sub-channels on either side of the island are represented by the parallel impedances Z_1 and Z_2 discussed above. The load is represented by a variable resistance, R_L, that is tuned to maximize its rate of energy dissipation. The basin is represented by the capacitive impedance, $1/i\omega C_B$, with $C_B = A_B/\rho g$. Since the basin capacitance is effectively in series with the impedances, Z_{M1} and Z_{M2}, of the main channel, these are lumped together in the circuit of Fig. 2a as $Z_B = R_M + i(\omega L_M - (\omega C_B)^{-1})$, where $R_M = R_{M1} + R_{M2}$ and $L_M = L_{M1} + L_{M2}$. It is convenient to express this as $Z_B = R_M + i\omega L_M(1 - \beta_M)$. As discussed below, $\beta_M = (\omega^2 L_M C_B)^{-1}$ is a parameter that controls one of the resonances of the system.

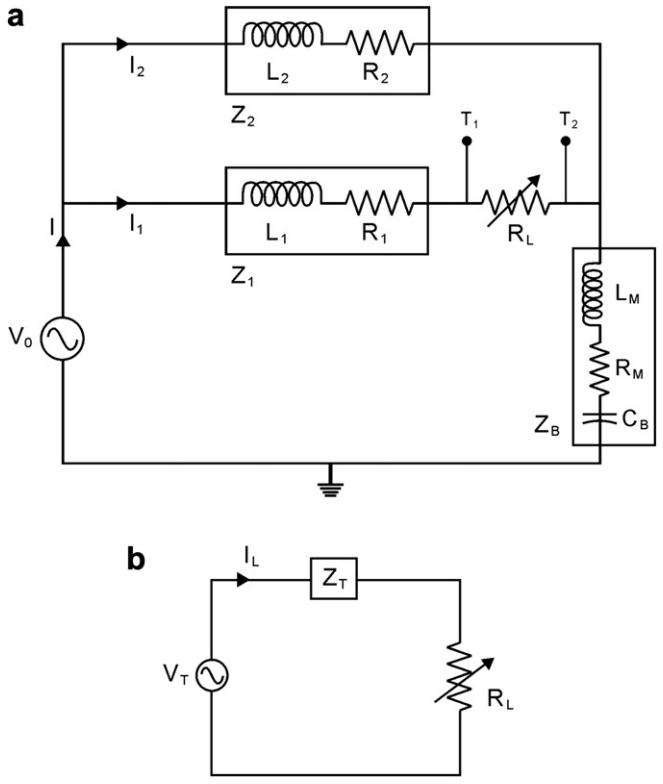

Fig. 2. (a) Electric circuit analogue to the flow configuration of Fig. 1. (b) Thévenin equivalent circuit for the load resistance, R_L.

2.1. Maximum extractable power

The first step in determining the maximum power is to apply Thévenin's theorem [16] to reduce the circuit of Fig. 2a to its equivalent circuit for the load resistance, R_L, as illustrated in Fig. 2b. The Thévenin voltage, V_T, is determined as the open circuit voltage at terminals T_1 and T_2 and is given by

$$V_T = \frac{Z_2 V_0}{Z_2 + Z_B}. \tag{4}$$

The Thévenin impedance, Z_T, is the equivalent impedance seen at T_1 and T_2 with the voltage source in the circuit of Fig. 2a shorted out. Since Z_1 then appears in series with the parallel combination of Z_B and Z_2, the Thévenin impedance is

$$Z_T = Z_1 + \frac{Z_2 Z_B}{Z_2 + Z_B}. \tag{5}$$

With I_L denoting the electric current in the circuit of Fig. 2b, the average power dissipated in the load resistance is given by

$$\langle P \rangle = \frac{1}{2} R_L |I_L|^2 = \frac{R_L |V_T|^2}{2|Z_T + R_L|^2}. \tag{6}$$

To maximize the dissipation in the load, the maximum power transfer theorem [16] requires that $R_L = |Z_T|$. With $Z_T = |Z_T| \exp i\phi$, the average extractable power then has an upper limit given by

$$\langle P \rangle_{\max} = \frac{|Z_T||V_T|^2}{2|Z_T + |Z_T||^2} = \frac{|V_T|^2}{4(1+\cos\phi)|Z_T|}. \tag{7}$$

It is evident from the circuit of Fig. 2a that, as the impedance of the free channel tends to zero, the impeded channel is shorted out ($V_T = 0$), and the available power vanishes to zero.

Defining the non-dimensional parameters

$$(\zeta_1, \zeta_2) = \left(\frac{Z_B}{Z_1}, \frac{Z_B}{Z_2}\right) \tag{8}$$

(4) and (5) can be written as

$$V_T = \frac{V_0}{(1+\zeta_2)} \tag{9}$$

and

$$Z_T = Z_1 \frac{(1+\zeta_1+\zeta_2)}{(1+\zeta_2)}, \tag{10}$$

respectively. Flows in the two sub-channels are coupled by the impedance Z_B. The limit $Z_B \to 0$, represents an infinite basin with negligibly short sections for the undivided main channel. In this limit, $(\zeta_1, \zeta_2) = 0$, and (9) and (10) reduce to $Z_T = Z_1$ and $V_T = V_0$, so that the flows in the two sub-channels are driven independently by the same tidal forcing. The extractable power (7) then reduces to $\langle P \rangle_{\max 1} = V_0^2/(4(1+\cos\phi_1)|Z_1|)$, where $\phi_1 = \mathrm{Arg}\, Z_1$. Here $\langle P \rangle_{\max 1}$ represents the power potential of the impeded channel in isolation, i.e., connecting two large basins and driven by a sea level difference, a, across its ends.

Making use of (9) and (10), the maximum average power (7) may be written in non-dimensional form,

$$\frac{\langle P \rangle_{\max}}{\langle P \rangle_{\max 1}} = \frac{C}{|1+\zeta_2| \cdot |1+\zeta_1+\zeta_2|}, \tag{11}$$

where $C = (1+\cos\phi_1)/(1+\cos\phi)$. The right hand side of (11) represents a scaling factor that relates the power potential of the impeded sub-channel embedded within the split-channel configuration to the power of this channel in isolation. This scaling will be less than unity in many instances as the presence of the parallel free channel allows flow to be diverted away from the turbine fence, thus reducing the available power [9].

Eq. (7) for the extractable power, along with the corresponding non-dimensional form (11), is the central result of this analysis. These relations express the maximum average extractable power in terms of the forcing at the mouth and physical properties of the channel and basin in the natural, undisturbed state. It is important to note that this quantity represents an upper bound on the available power. As such, it does not take into account the electrical and mechanical losses associated with operation of the turbines, nor fluid mechanical losses due to drag on supporting structures and mixing of streams in the wake. The response in (11) is governed by the two complex non-dimensional parameters defined in (8). A few special cases are considered below in Section 3.

The preceding results may be extended to the case of N sub-channels in which the flow in one of the sub-channels is impeded. Let Z_n represent the impedance of sub-channel n, and assume, as above, that the turbine fence is placed in sub-channel 1. Then the extractable power is again given by (7), provided that Z_2 in Eqs. (4) and (5) is replaced by Z_{EQ}, where $Z_{EQ} = (\sum_{n=2}^{N} Z_n^{-1})^{-1}$ is the equivalent impedance of the $N-1$ free sub-channels.

2.2. Flow modification

Other quantities of interest may be readily derived from the equivalent circuit. In particular, since the load current, I_L, of Fig. 2b is identical to the branch current, I_1, of Fig. 2a, the fractional reduction of the flow in the impeded sub-channel at maximum power is given by

$$F_1 \equiv \frac{|I_1|_{R_L=|Z_T|}}{|I_1|_{R_L=0}} = \frac{|Z_T|}{|Z_T + |Z_T||}, \tag{12}$$

which simplifies to,

$$F_1 = \frac{1}{\sqrt{(2+2\cos\phi)}}. \tag{13}$$

It can be shown that $ReZ_T \geq 0$, provided that all the resistances are dissipative, $(R_1, R_2, R_B) \geq 0$. Hence, $0 \leq \cos\phi \leq 1$, and we must have $0.5 \leq F_1 \leq 2^{-1/2}$. At maximum power, the transport in the impeded channel is reduced to between 50% and 71% of its magnitude in the undisturbed state. The lower limit applies if the Thévenin impedance is purely resistive, while the upper limit applies if this impedance is purely reactive. These limits are similar to those of the single channel case with linear friction [2,5].

The change in the transport of the free sub-channel can be found by noting that the parallel branches of the circuit of Fig. 2a have the same voltage drop, so that $I_2 Z_2 = I_1(Z_1 + R_L)$. From the equivalent circuit of Fig. 2b, $I_1 = I_L = V_T/(Z_T + R_L)$. Thus the fractional change in the transport of the free sub-channel is given by

$$F_2 \equiv \frac{|I_2|_{R_L=|Z_T|}}{|I_2|_{R_L=0}} = F_1 \frac{|Z_1 + |Z_T||}{|Z_1|}. \tag{14}$$

This quantity is not constrained to be greater than one. Although the introduction of turbines may be expected to divert flow from the impeded sub-channel into the free sub-channel, the transport in the latter may nevertheless decrease if the total transport $(I = I_1 + I_2)$ decreases sufficiently. It is straightforward to show that at maximum power the total transport changes by the factor,

$$F \equiv \frac{|I|_{R_L=|Z_T|}}{|I|_{R_L=0}} = F_1 \frac{|Z_1 + Z_2 + |Z_T||}{|Z_1 + Z_2|}. \tag{15}$$

The tidal range in the basin is subject to the same fractional change as that given by (15).

3. Limits and special cases

In general, the power in the split channel problem depends on two complex non-dimensional parameters so that there is effectively a four-dimensional parameter space governing the response. A few illustrative cases are considered for which the parameter space governing the response is effectively two-dimensional. Firstly, it is demonstrated that the results presented above are consistent with previous results for a single channel.

3.1. Single channel limit

The single channel limit is recovered by having the cross-sectional area of the free sub-channel tend to zero such that $Z_2 \to \infty$. As a result, the Thévenin voltage (4) simplifies to $V_T = V_0$ and the impedance (5) becomes $Z_T = Z_1 + Z_B = R + i\omega L(1-\beta)$. Here $R = R_1 + R_M$ and $L = L_1 + L_M$ represent the resistance and inductance, respectively, of the entire channel from the mouth to the basin. The channel-basin geometry parameter, $\beta = (\omega^2 L C_B)^{-1} = g/\omega^2 c A_B$, represents the square of the ratio of the Helmholtz resonance frequency to the forcing frequency [3,4]. Accordingly, $|Z_T|\cos\phi = R$, and $|Z_T| = \omega L(\delta^2 + (1-\beta)^2)^{1/2}$, where $\delta = R/\omega L$ is the non-dimensional friction parameter. This parameter reduces to $\delta = r/\omega$ if the background friction coefficient is taken as constant along the channel. The maximum average power from (7) is then

$$\langle P\rangle_{\max} = \frac{V_0^2/\omega L}{4\left(\delta + \left(\delta^2 + (1-\beta)^2\right)^{1/2}\right)} \tag{16}$$

which simplifies to $\langle P\rangle_{\max} = V_0^2/8R$ at Helmholtz resonance ($\beta = 1$). The expression (16) is a generalization of Eq. (34) of Blanchfield et al. [3] to allow for channel friction, and it obtained by combining Eqs. (17) and (18) of [5]. The dimensionalizing factor, $V_0^2/\omega L = \rho(ga)^2/c\omega$, is consistent with previous studies [1,3,5].

3.2. Resistive impedances

If flow acceleration in the channels is neglected and the basin is assumed to be of infinite extent, then the impedances are purely resistive and $(Z_1, Z_2, Z_B) = (R_1, R_2, R_M)$. As indicated by the solution for the single channel (16), the condition for friction in the impeded channel to dominate acceleration is $\delta \gg |1-\beta|$, which reduces to $\delta \gg 1$ if the basin is of infinite extent ($\beta = 0$). Thus the resistive limit applies if the tidal periodicity is long compared to the time scale for frictional decay for each channel. Atwater and Lawrence [9] considered this limit, allowing for quadratic drag law. As they optimize with respect to extraction efficiency rather than extracted power, this precludes a quantitative comparison with results from the present analysis. However, as noted below, it is apparent that there is at least qualitative agreement in the salient results based on these two approaches.

In the resistive case, the non-dimensional impedance ratios, $(\zeta_1, \zeta_2) = (R_M/R_1, R_M/R_2)$, are both real, positive-definite quantities. The Thévenin impedance (5) is also real so that $\cos\phi = 1$, and power ratio (11) reduces to,

$$\frac{\langle P\rangle_{\max}}{\langle P\rangle_{\max 1}} = \frac{1}{(1+\zeta_2)(1+\zeta_1+\zeta_2)}. \tag{17}$$

where $\langle P\rangle_{\max 1} = V_0^2/8R_1$. The contour plot of (17) presented in Fig. 3a shows that, even for moderate values of the parameters, the power that is available from the impeded channel is reduced considerably within the split channel configuration. Moreover, there is markedly asymmetrical dependence of the power on the non-dimensional parameters. In particular, for fixed ζ_2 the right hand side of (17) scales as ζ_1^{-1} at large ζ_1, whereas at large ζ_2 it scales as ζ_2^{-2}. This latter limit corresponds to shorting out the impeded sub-channel ($R_2 \to 0$). Consequently, and as might generally be expected, it is advantageous from the standpoint of power extraction to place the turbine fence in the sub-channel with the least natural resistance, thereby minimizing ζ_2. It is evident that this also holds in the results of [9] (their Fig. 3). The point at the origin of Fig. 3a corresponds to the limit $Z_B = R_M = 0$ wherein the impeded and free sub-channels are decoupled and the available power reduces to $\langle P\rangle_{\max}/\langle P\rangle_{\max 1} = 1$.

As mentioned above, in the resistive limit the transport in the impeded sub-channel at maximum power is reduced to 50% of its value in the undisturbed state. Since $F_1 = 0.5$, we have from (14) that the fractional change in the transport in the free sub-channel is $1 + 0.5\zeta_1/(1+\zeta_2) > 1$. Thus the turbine fence always increases the transport in the free sub-channel in the resistive limit, also in general agreement with the results of [9].

3.3. Reactive impedances

In the reactive limit, bottom drag is neglected and the resistive components of the impedances are set to zero such that $(Z_1, Z_2, Z_B) = i\omega(L_1, L_2, L_M(1-\beta_M))$. The impedance ratios (8) are again real quantities, but of indefinite sign. They can be expressed as $(\zeta_1, \zeta_2) = (\beta_1(\beta_M^{-1} - 1), \beta_2(\beta_M^{-1} - 1))$, where $\beta_1 = (\omega^2 L_1 C_B)^{-1}$ and $\beta_2 = (\omega^2 L_2 C_B)^{-1}$ are channel-basin geometry parameters for the

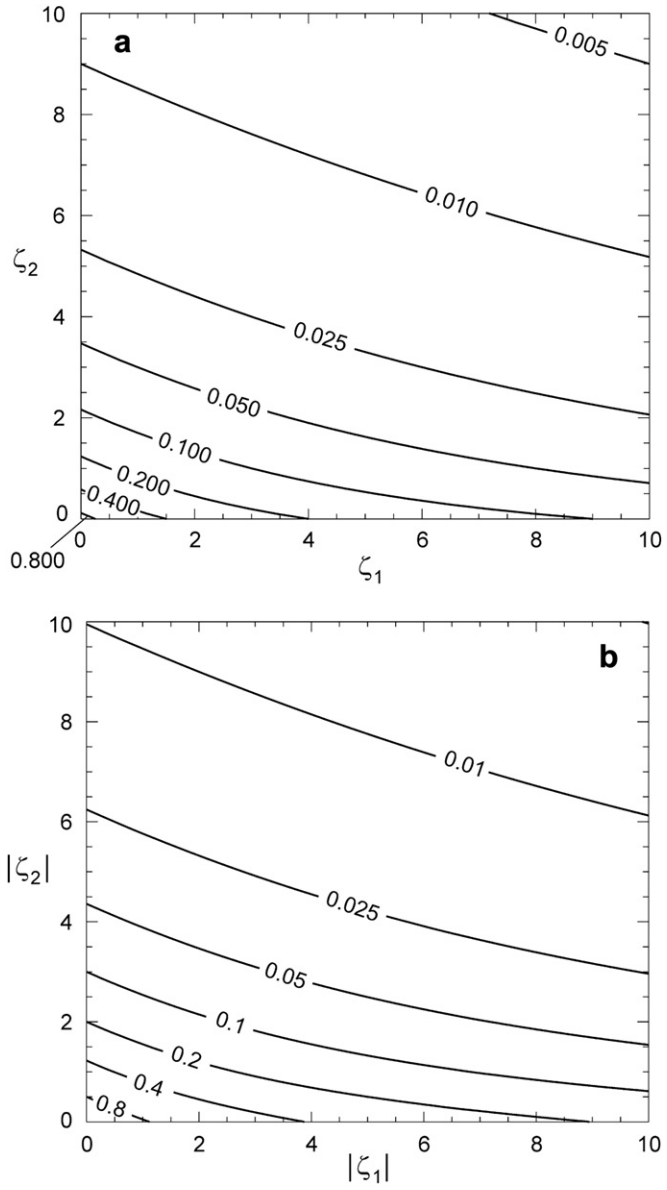

Fig. 3. Scaling factor for the extractable power in (a) the resistive case of section 3.2, and (b) the mixed impedance case of section 3.4. Only the upper right quadrant of the $(|\zeta_1|, |\zeta_2|)$ plane is shown in (b) as the parameters are purely imaginary and $\langle P(\zeta_1, \zeta_2)\rangle_{\max} = \langle P(-\zeta_1, -\zeta_2)\rangle_{\max}$.

impeded and free sub-channels, respectively. Substituting into (11) and noting that $\cos\phi = \cos\phi_1 = 0$ in the reactive limit, the maximum average extractable power may be expressed in terms of these parameters as,

$$\frac{\langle P\rangle_{\max}}{V_0^2/4\omega L_1} = \frac{1}{\left|1+\beta_2\left(\beta_M^{-1}-1\right)\right|\cdot\left|1+(\beta_1+\beta_2)\left(\beta_M^{-1}-1\right)\right|}. \tag{18}$$

The Helmholtz resonance condition associated with the undivided sections of the main channel is $\beta_M = 1$, which amounts to setting $Z_B = 0$. As mentioned above, the sub-channels are decoupled in this limit and the power is simply $\langle P\rangle_{\max} = V_0^2/4\omega L_1$. Two additional resonance conditions are evident from (18):

$$\beta_2 = \left(1-\beta_M^{-1}\right)^{-1} \tag{19a}$$

$$\beta_1+\beta_2 = \left(1-\beta_M^{-1}\right)^{-1}. \tag{19b}$$

These correspond to Helmholtz resonances associated with the free sub-channel and the combination of the impeded and free sub-channels, respectively. It may be noted that $\beta_2 \to 0$ in the single channel limit, and the resonance condition (19b) reduces to $\beta^{-1} = \omega^2 C_B(L_1+L_M) = 1$ as discussed above.

3.4. Mixed impedances

An additional case which simplifies to two governing non-dimensional parameters occurs as the impedances of the sub-channels are purely resistive while Z_B is purely reactive. This limit may be relevant to situations where the sub-channels are shallow, while the basin is of finite area and/or the undivided sections of the main channel are relatively deep. The governing non-dimensional parameters (8) in this case are purely imaginary and of indefinite sign, $(\zeta_1, \zeta_2) = i\omega L_M(1-\beta_M)(R_1^{-1}, R_2^{-1})$. The non-dimensional power ratio evaluated from (11) is presented in Fig. 3b. The pattern is qualitatively similar to that of the resistive case shown in Fig. 3a. For given values of the parameters, the extractable power, however, is relatively larger in the present case, except at the origin which corresponds to the resonance condition, $\beta_M = 1$. In this limit, the two sub-channels are independent and the maximum average power is $\langle P\rangle_{\max} = V_0^2/8R_1$, similar to the resistive case with $R_M = 0$.

3.5. A simple example

Lastly, an idealized example is presented to illustrate calculation of the available power through application of the preceding results. In this case, it is assumed that the impeded and free sub-channels each have lengths of 5 km, nominal depths of $H = 15$ m, and constant cross-sectional areas of $A_1 = 0.75\times10^4$ m^2 and $A_2 = 1.5\times10^4$ m^2, respectively. The lengths of the main channel on either side of the island are assumed to be sufficiently short that the impedance of these regions can be neglected ($R_M = L_M = 0$), so that $Z_B = -i/\omega C_B = -i\rho g/\omega A_B$. Effects of varying the basin area, A_B, will be considered. At the mouth, an M_2 tidal forcing ($\omega = 1.405\times10^{-4}$ s^{-1}) is assumed with an amplitude of 1 m. The linear drag coefficient is chosen so that energy dissipation over a tidal cycle due to linear drag matches that of a quadratic drag law. If the tidal current in the channels has the form $u = u_0\cos\omega t$, this gives $r = 8/3\pi C_D u_0/H \approx 0.85 C_D u_0/H$. With a magnitude for the current of $u_0 = 1$ m s^{-1}, and a quadratic drag coefficient, $C_D = 0.0025$, we have $r \approx 1.4\times10^{-4}$ s^{-1} for both sub-channels. Given these values and taking $\rho = 1025$ kg m^{-3} as the density of seawater, the impedance of the impeded sub-channel is $Z_1 = \rho l_1(r+i\omega)/A_1 = 0.096 + i0.096$, while for the free sub-channel, $Z_2 = 0.048 + i0.048$. Background friction and flow acceleration thus make equal contributions to the channel impedances in this case.

Fig. 4a presents the available power determined from (7) as a function of the basin area. This is compared with the power, determined from (16), for a single channel with impedance Z_1. Variation of the geometry parameters for the sub-channels (β_1 and β_2) is given in Fig. 4b, while the fractional change in the sub-channel transports is presented in Fig. 4c. Since $L_M = 0$, the resonance conditions (19a,b) are $\beta_2 = 1$ and $\beta_1+\beta_2 = 1$, respectively.

For small to medium size basins (hence relatively large basin impedance), the maximum available power is reduced significantly by the presence of the free sub-channel. For example, with $A_B = 5\times10^8$ m^2, the maximum average power from the impeded sub-channel is 25 MW. This compares with 124 MW for the single channel case with a basin of similar area. The extractable power drops from 25 MW to 9 MW if L_1 and L_2 are arbitrarily set to zero, so

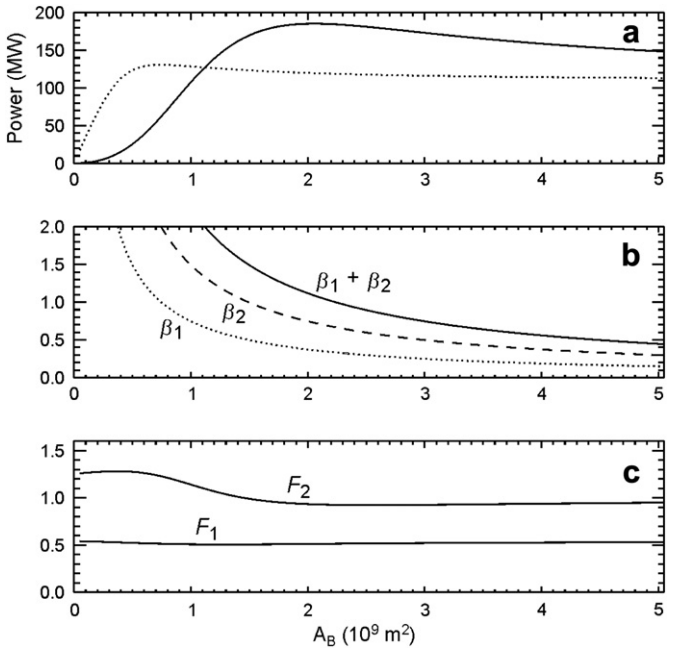

Fig. 4. Results from the example discussed in Section 3.5. (a) Variation of the maximum extractable power with basin area. The solid line is for the split channel, while the dotted line is the corresponding single channel case. (b) Dependence of the channel-basin parameters with varying basin area. (c) Fractional change in the magnitude of the transport in the two sub-channels with varying basin area.

it is clear that flow acceleration has an important influence on the power in this case. The transport is reduced in the impeded sub-channel to 52% of its magnitude in the natural state while the flow in the free sub-channel increases by about 28%. On the other hand, the total transport (not shown) remains essentially unchanged.

As the basin area increases, the power available from the impeded sub-channel increases and eventually surpasses that of the corresponding single channel case. There is a broad peak in the power that occurs close to the combined channel resonance condition (19b), $\beta_1 + \beta_2 = 1$. The response here is heavily damped such that there is no distinguishable peak at $\beta_2 = 1$. The peak power in the single channel case occurs close to $\beta_1 = 1$ and is also very broad due to the damping.

For continued increases in basin area, the power available from the impeded sub-channel tends asymptotically to that of the single channel case with $\beta_1 = 0$. This is limit $Z_B \to 0$ for which the free and impeded sub-channels are decoupled. The magnitude of the flow in the free sub-channel dips slightly below its value in the undisturbed state ($F_2 < 1$) with increasing basin area. Eventually, as A_B becomes very large, F_2 tends to unity.

4. Summary and discussion

The problem of estimating the extractable power from tidal motions has received increasing attention over the past decade. A basic theory has been developed that applies to relatively simple flow configurations. Coastal regions, on the other hand, are frequently characterized by complex networks of interconnected channels. While recourse to numerical modelling is one option in such circumstances, simple analytical approaches can often be instructive and help guide and interpret numerical results (e.g., [17]). A canonical problem in this regard is that of a tidal channel that is split into two branches by an island, with energy extraction devices deployed in one of the sub-channels [9,10]. The other sub-channel is assumed to be left free for other purposes, or to minimize the impacts of energy extraction on the environment.

In the present paper, the split channel problem has been considered in terms of an equivalent electrical circuit. This approach represents a basic linear theory that allows incorporation of inertial effects associated with flow acceleration in the channels and mass storage in the basin. Once the circuit analogue is determined, the maximum extractable power is obtained by following the standard approach of first reducing the circuit to its Thévenin equivalent and then applying the maximum power transfer theorem. This method of solution is limited, however, to energy extraction from only one sub-channel.

Analysis of the split channel problem leads to an expression (7) for the maximum average power in terms of the impedances of various sections of the channels. This maximum represents an upper bound on the available power; various losses will inevitably reduce the power that is realized in any given setting from this maximum. The expression (7) may be generalized to the case of a multiple branching channel, provided that the impedance of the single free channel is replaced with the equivalent impedance of the multiple parallel free channels. In non-dimensional form, the analysis shows that the power generally depends on two complex non-dimensional parameters, regardless the number of free sub-channels.

At maximum power, the results show that the transport in the impeded channel is reduced to between 50% and 71% of its value in the undisturbed state, depending on the underlying momentum balance in the channel. Interestingly these are the same limits as in the single channel case [5]. This result is consistent with numerical studies [10,17] that find the transport in the impeded channel in a branching network reduced at maximum power to approximately 58% of its magnitude in the undisturbed state. This reduction (58%) is the theoretical value for a single channel in the resistive limit with a quadratic drag law [1].

The assumption of linear bottom friction is perhaps the least realistic aspect of the equivalent circuit approach. Drag coefficients must be specified and these depend linearly on the magnitude of the flow through the channels. However, these flows are affected by the extraction of energy which will in turn modify the drag coefficients. A simple ad hoc way to take this into account is to make use of the fact that, at maximum power, flow in the impeded sub-channel is reduced to 50–71% of its magnitude in the undisturbed state. As a first approximation, the resistance of the impeded sub-channel could then be reduced to say 60% of its value based on the undisturbed flow. Similarly, the resistance of the free sub-channel could be augmented by taking account of the flow modification expected from (14). In cases where friction dominates the momentum balance, quadratic friction can then be expected to increase the available power over a linear drag law.

It is interesting to consider application of this approach to account for the effects of quadratic drag to the resistive case. The estimated power potential of the impeded channel in isolation would then be modified such that,

$$P_{\max 1} = \frac{1}{8}\,\frac{V_0^2}{(0.6R_1)} \approx 0.21\frac{V_0^2}{R_1} = 0.21\rho g a Q_{\max}. \tag{20}$$

The channel resistance of the impeded channel in (20) has been reduced to 60% of its value in the undisturbed case, thus anticipating the reduced transport at maximum power. This factor is virtually the same as the reduction to 58% of the transport from the undisturbed state in a channel connecting two large basins under quadratic drag [1]. On the right hand side of (20), $Q_{\max} = V_0/R_1$ represents the amplitude of the transport of the impeded channel under linear friction when driven by sea level difference a. The expression on the right hand side of (20) agrees closely with results given in [1] for the power potential of a frictional channel connecting two large basins

with Q_{max} representing the peak transport in the undisturbed state. The power potential of the impeded channel within the split channel configuration would be approximated then as the product of $0.21V_0^2/R_1$ with the scaling factor, $S = [(1+\zeta_2)(1+\zeta_1+\zeta_2)]^{-1}$, that is plotted in Fig. 3a. The influence of nonlinear drag will be to increase (reduce) ζ_1 (ζ_2) within this scaling factor. Since these are offsetting influences, linear theory indicates that for moderate values of these parameters ($0 < \zeta_1 < 4.5, 1 < \zeta_2 < 10$) the adjustment to S is small (<10% change) and could be ignored.

The electric circuit approach may be extended to more complex flow configurations. Application of the method requires estimation of the natural impedance of various branching channels. If results from a regional numerical tidal model are available, then the impedance for a given channel can be determined simply as the ratio of the pressure difference across the ends of the channel to the volume transport. Likewise, the impedance presented by a basin may be determined numerically as the ratio of the pressure at the entrance to the transport into the basin. It is possible in this way to overcome the restriction of small basin size and include the effects of losses associated with radiation into the basin (e.g., [18]).

The split channel problem is similar in certain respects to that of a channel that is partially spanned by a turbine fence [6–8]. In each case, power is maximized in a configuration that allows the flow to bypass the energy extraction devices. Future exploration of this analogy could be useful as a means of understanding the influence of non-linear bottom drag and momentum advection on the available power.

Acknowledgements

The author is grateful to Mike Foreman for discussions and to two reviewers for providing useful comments. Rosalie Rutka assisted with the figures.

References

[1] Garrett C, Cummins P. The power potential of tidal currents in channels. Proceedings of the Royal Society of London A 2005;461:2563–72.
[2] Garrett C, Cummins P. Generating power from tidal currents. Journal of Waterway, Port, Coastal, and Ocean Engineering 2004;130:114–8.
[3] Blanchfield J, Garrett C, Wild P, Rowe A. The extractable power from a channel linking a bay to the open ocean. Proceedings of the Institution of Mechanical Engineers, Part A: Journal of Power and Energy 2008;222(A3): 289–97.
[4] Karsten R, McMillan J, Lickley M, Haynes R. Assessment of tidal current energy in the Minas Passage, Bay of Fundy. Proceedings of the Institution of Mechanical Engineers, Part A: Journal of Power and Energy 2008;222(A5): 493–507.
[5] Cummins P. On the extractable power from a tidal channel. Journal of Waterway, Port, Coastal, and Ocean Engineering 2012;138:63–71.
[6] Garrett C, Cummins P. The efficiency of a turbine in a tidal channel. Journal of Fluid Mechanics 2007;588:243–51.
[7] Vennell R. Tuning turbines in a tidal channel. Journal of Fluid Mechanics 2010; 663:253–67.
[8] Vennell R. Tuning tidal turbines in-concert to maximise farm efficiency. Journal of Fluid Mechanics 2011;671:587–604.
[9] Atwater J, Lawrence G. Power potential of a split tidal channel. Renewable Energy 2010;35:329–32.
[10] Polagye B, Malte P. Far-field dynamics of tidal energy extraction in channel networks. Renewable Energy 2011;36:222–34.
[11] Miles J. Resonant response of harbours: an equivalent-circuit analysis. Journal of Fluid Mechanics 1971;46:241–65.
[12] Rainey R. The optimum position for a tidal power barrage in the Severn estuary. Journal of Fluid Mechanics 2009;636:497–507.
[13] Garrett C, Greenberg D. Predicting changes in tidal regime: the open boundary problem. Journal of Physical Oceanography 1977;7:171–81.
[14] Shapiro G. Effect of tidal stream power generation on the region-wide circulation in a shallow sea. Ocean Science 2011;7:165–74.
[15] Lighthill M. Waves in fluids. Cambridge University Press; 1978.
[16] Dorf R, Svoboda J. Introduction to electric circuits. 8th ed. John Wiley & Sons Inc; 2010.
[17] Sutherland G, Foreman M, Garrett C. Tidal current energy assessment for Johnstone Strait, Vancouver Island. Proceedings of the Institution of Mechanical Engineers, Part A: Journal of Power and Energy 2007;221(A2): 147–57.
[18] Cummins P, Karsten R, Arbic B. The semi-diurnal tide in Hudson Strait as a resonant channel oscillation. Atmosphere-Ocean 2010;48:163–76.